



Published in final edited form as:

*J Biomed Mater Res A*. 2008 September ; 86(3): 617–626. doi:10.1002/jbm.a.31649.

## SURFACE CHEMISTRY INFLUENCE IMPLANT MEDIATED HOST TISSUE RESPONSES

Shwetha Kamath<sup>1</sup>, Dhiman Bhattacharyya<sup>2</sup>, Chandana Padukudru<sup>1</sup>, Richard B. Timmons<sup>2</sup>, and Liping Tang<sup>1,\*</sup>

<sup>1</sup>Bioengineering Department, University of Texas at Arlington, PO Box 19138, Arlington, TX 76019-0138

<sup>2</sup>Chemistry and Biochemistry Department, University of Texas at Arlington, PO Box 19065, Arlington, Texas 76019-0065

### Abstract

Implant-mediated fibrotic reactions are detrimental to the performance of encapsulated cells, implanted drug release devices and sensors. To improve the implant function and longevity, research has emphasized altering cellular responses. Although material surface functional groups have been shown to be potent in affecting cellular activity in vitro and short term in vivo responses, these groups appear to have little influence on long-term in vivo fibrotic reactions, possibly as a result of insufficient interactions between recruited host cells and functional groups on the implants. To maximize the influence of functionality on cells, and to mimic drug release microspheres, functionalized micron-sized particles were created and tested for their ability in modulating tissue responses to biomaterial implants. In this work, the surfaces of polypropylene particles were controllably coated with four different functional groups, specifically –OH, –NH<sub>2</sub>, –CF<sub>x</sub> and –COOH, using a radio frequency glow discharge plasma polymerization technique. The effect of these surface functionalities on host tissue responses were then evaluated using a mice subcutaneous implantation model. Major differences were observed in contrasting tissue response to the different chemistries. Surfaces with –OH and –NH<sub>2</sub> surface groups induced the thickest fibrous capsule accompanied with the greatest cellular infiltration into the implants. In contrast, surfaces with –CF<sub>x</sub> and –COOH exhibited the least inflammatory/fibrotic responses and cellular infiltrations. The present results clearly demonstrate that, by increasing the available functionalized surface area and spatial distribution, the effect of surface chemistry on tissue reactivity can be substantially enhanced.

### Keywords

Surface modification; inflammation; fibrosis; microsphere; plasma polymerization

## INTRODUCTION

Implantable devices are increasingly important in the practice of modern medicine. Despite being chemically inert, non-immunogenic and non-toxic, most biomaterial implants cause acute inflammatory responses. A sequence of events initiated with an acute inflammatory response and subsequently leading to granulation tissue development, and finally fibrous capsule development, is known to occur. [1] Such excessive fibrotic responses have been

\*Correspondence to Liping Tang, Ph.D., Biomedical Engineering program, University of Texas at Arlington, P.O. Box 19138, Arlington, TX 76019-0138. fax: 817-272-2251; ltang@uta.edu.

shown to lead to failure of many types of medical implants, including implantable sensors, encapsulated cells and drug release devices.[2–6] Specifically, the formation of collagenous capsule acts as a diffusion barrier for an encapsulated drug to transport into circulation and for oxygen and nutrient of the surrounding tissue to move to encapsulated cells.[3–6] Obviously, these findings raise the important question of how the body recognizes and prompt fibrotic reactions to implanted biomaterials.

In an attempt to address this question, the sequence of responses to material implants, involving shorter time scales, have been studied in many laboratories. Shortly after implantation (seconds to minutes), biomaterials spontaneously acquire a layer of host proteins. A few hours later (4 to 8 hours), host cells (mostly phagocytes) start to accumulate on implant surfaces. In a few days, biomaterial implants are surrounded by a prominent layer of fibrotic tissue composed of fibroblasts and collagen. [7–10] Since biomaterials quickly and spontaneously acquire a layer of host proteins prior to interacting with host cells, it is highly probable that the types and state of adsorbed proteins are critical determinants of reactions to biomaterial implants.[11–17]

The physical and chemical properties of implant materials have been shown to affect protein adsorption and cellular responses under in vitro conditions.[18] To generate surfaces with better tissue compatibility, many surface modification techniques, including physical modifications, chemical modifications, and radiation,[18,19] have been developed to alter the physical and chemical characteristics of the biomaterials. The modifications of material surface properties, including wettability, chemistry, domain composition and morphology, have been shown to influence protein adsorption and subsequent cellular responses to biomaterials in vitro. [20–31] Surface functionality has also been shown to alter biomaterial-mediated acute inflammatory responses in vivo.[26,32,33] However, these modifications of surface chemistry exert minimal influence on chronic fibrotic responses in vivo. [26,34,35,36]

We speculate that the relatively ineffectiveness of surface functionality on long-term in vivo cellular responses may simply reflect insufficient cell:surface interactions. Specifically, in an in vitro setting, cells are seeded on top of functional group and surface functionality, thus, exerting maximal effect on cellular responses. On the other hand, in an in vivo environment, the functional groups on non-porous implants can only interact with the first layer of the cells which represent only a small portion of the surrounding cells/tissue. These relatively poor cell-functional group interactions thus minimize the effect of surface functionality on cellular responses. Thus we hypothesized that possibly the influence of implant surface chemistry may be substantially enhanced by increasing the interaction between functional groups and cells in applications such as tissue scaffolds and drug releasing microspheres. To test this hypothesis, we have examined, in vivo, response to microspheres bearing different, molecularly tailored, surface functionalities. Spherical particles were chosen for this purpose to maximize the surface to volume ratio of the implants and also to mimic microspheres used for controlled drug release.

Only a small number of surface modification techniques have been established to covalently link different functional groups on particles. Our laboratory has recently developed a modified Radio Frequency Glow Discharge (RFGD) technique to functionalize a wide variety of micro [37], and more recently, nanosized, spheres [38]. Additionally, using a pulsed plasma technique, we have previously shown that we can effectively control the film chemistry obtained from a given monomer undergoing polymerization via simple variations in the plasma duty cycles employed. This film chemistry control can be used to permit retention of normally reactive functional groups in monomers polymerized under plasma

conditions [39,40] and this technology has been successfully employed in variety of biomaterial applications [37, 41–44].

To examine the influence of surface chemistry on foreign body responses triggered on implantation, we employed polypropylene particles coated with -OH, -NH<sub>2</sub>, -CF<sub>x</sub> and -COOH functionalities. After subcutaneously implantation in mice for two weeks, the implants and their surrounding tissues were recovered for histological analyses. The results obtained clearly show that surface functionality on microspheres has a profound effect on tissue response, as revealed by capsule thickness and cell infiltration around the particle implants.

## MATERIALS AND METHODS

### Materials

Polypropylene microspheres, of uniform 35 micron diameter, were obtained from Polysciences, Inc (Warrington, Pa). Ethylenediamine, (NH<sub>2</sub>CH<sub>2</sub>CH<sub>2</sub>NH<sub>2</sub>), di(ethylene glycol) vinyl ether [CH<sub>2</sub>=CH(OCH<sub>2</sub>CH<sub>2</sub>)<sub>2</sub>OH], hereafter EO2V, and vinyl acetic acid, CH<sub>2</sub>=CHCH<sub>2</sub>COOH, (hereafterVAA), were obtained from Sigma Chemical Company (St. Louis, MO) and were of the highest purities available. Perfluorohexane, C<sub>6</sub>F<sub>14</sub>, obtained from the 3M Company (Minneapolis, MN) consisted primarily of the n-isomer (>90%), the remainder being C<sub>6</sub>F<sub>14</sub> branched isomers. Each monomer was out-gassed repeatedly, using freeze thaw cycles, prior to use.

Primary antibody against CD11b was purchased from Santa Cruz Biotechnology Inc (Santa Cruz, CA). Texas Red was from Jackson ImmunoResearch laboratories, Inc. (West Grove, PA).

### Modification of polymeric surfaces

The polypropylene micron size particles were surface functionalized using plasma polymerization of four different monomers. These monomers were selected to provide a diverse variety of chemistries ranging from uncharged hydrophobic (C<sub>6</sub>F<sub>14</sub>) and hydrophilic (EO<sub>2</sub>V), to cationic (VAA) and anionic (NH<sub>2</sub>C<sub>2</sub>H<sub>4</sub>NH<sub>2</sub>) hydrophilic surfaces. A home built custom reactor, capable of continuous 360° rotation during the plasma deposition was employed to overcome the tendency for particle aggregation and thus promote more uniform polymer film coverage of the substrates [37,38]. One gram samples of the particles were coated in each run. The polypropylene microspheres were soaked in ethanol, followed by prolonged vacuum drying prior to the plasma treatment. Pulsed plasmas were employed with all four monomers during the polymer film coating process. Preliminary studies involved maximizing the polymer functional group densities, via plasma duty cycle and peak power input, consistent with providing films strongly grafted to the microspheres and sufficiently cross-linked to resist dissolution when immersed in aqueous solutions. After coating and before implantation, the microspheres were placed in a vacuum oven, set at 50°C, and pumped overnight to remove any monomers and/or low molecular weight oligomers adsorbed on these particles from the plasma process. The structure of the polymer films were determined using XPS and FT-IR spectroscopy and the wettability of the surfaces were measured using a static angle Rame-Hart sessile drop goniometer. These film characterization measurements were made on flat substrates coated in the plasma reactor under identical conditions to those employed with the polypropylene particles. Polished Si substrates were employed for the XPS and water contact angle measurements and KBr discs for the FT-IR determinations. Specific surface functionalities of interest obtained from these monomers were -OH (from EO<sub>2</sub>V); -NH<sub>2</sub> (from ethylenediamine); -CF<sub>x</sub>, primarily CF<sub>2</sub>, (from C<sub>6</sub>F<sub>14</sub>); and -COOH (from VAA). These test surfaces, having different degrees of

hydrophobicity, hydrophilicity and positive ( $\text{NH}_3^+$ ) and negative ( $\text{COO}^-$ ) charges, when immersed in pH 7 aqueous solutions, were selected based on the fact these surface properties have been shown to govern protein adsorption, retention and epitope exposure. Specifically, hydrophobic surfaces and positive charged surfaces are known to exhibit a high propensity to bind protein irreversibly. [26]

### **Animal implantation model**

The surface functionalized polypropylene particles were implanted subcutaneously in Balb/C mice (25 grams body weight) from Taconic Farms (Germantown, NY, USA). Polypropylene particles, without any surface modification but subjected to the ethanol wash/vacuum drying process, were employed as control samples. After implantation for 2 weeks, implant-bearing mice were sacrificed and the implants and the surrounding tissues were then frozen in OCT embedding media (Polysciences Inc., Warrington, PA) at  $-80^\circ\text{C}$  for histological and immuno-histochemical analyses.

### **Histological and immunohistochemical analyses**

Frozen tissues embedded in OCT compound (Polysciences Inc., Warrington, PA) were stored in plastic cryomoulds, at  $-80^\circ\text{C}$ . Ten  $\mu\text{m}$  thick sections were sliced using a Leica Cryostat (CM1850) and placed on poly-L-lysine coated slides. To assess the tissue responses to particle implants, some of these slides were H&E stained. To determine the extent of biomaterial-mediated inflammatory responses, immunohistological analyses for CD11b+ inflammatory cells were carried out on some tissue slides. These slides were rinsed in washing buffer and then blocked with 1% BSA solution by incubating for 40min at  $37^\circ\text{C}$ . After rinsing in PBS, tissue sections were then incubated with the primary antibody CD11b for 2 hrs at  $37^\circ\text{C}$ , using an appropriate dilution. This was followed by rinsing in PBS and then incubating with Texas red-conjugated rabbit anti-mouse CD11b at a dilution of 1:500 for 1hr at  $37^\circ\text{C}$ . Following rinse, the slide sections were ready for image analysis. Prolong gold antifade reagent (Molecular Probes, OR) was mounted on the samples after the experiment to preserve the fluorescence.

### **Microscopy and Image Analyses**

After preparation, sections were analyzed using a Leica fluorescence microscope (Leica Microsystems, Wetzlar, GmbH) equipped with a Nikon E500 Camera (8.4V, 0.9A, Nikon Corp., Japan). Microscopy and Image analysis was used to assess the extent of implant-mediated fibrotic responses by measuring the numbers of implant-associated cells and the distance of cell infiltration into particle implants. The numbers of implant-associated cells were calculated based on blue stained nuclei seen, using the H&E staining, in the fibrotic capsule surrounding the implant. The distance of cell infiltration was determined based on the penetration of the cells into the polymeric implant. Immunohistochemistry stains were done to quantify the densities of implant associated CD11b+ inflammatory cells.

### **Statistical analyses**

Statistical comparison (achieved on the basis of variable cell number, infiltration depth and thickness of capsule) was carried out according to Student t- test. Differences were considered statistically significant when  $p < 0.05$ .

## **RESULTS**

### **RFGD modified polypropylene particles with varying surface functionality**

To determine the possible role of specific surface properties in modulating tissue responses, we generated surface modifications using the four monomers noted above, and the RFGD

approach, to deposit thin polymeric films on the polypropylene particles. As noted above, these monomers provide four distinctly different surface chemistries on the particles as summarized in Table 1, which also lists the plasma deposition conditions employed with each monomer and the hydrophobic or hydrophilic character of the films based on the water contact angle measurements. The plasma condition column in Table 1 provides, in sequence: the ratio of plasma on to plasma off times (in ms), the peak input power in Watts, the monomer pressure, in millitorr, and the deposition time in minutes employed in the coating of each sample.

The actual film compositions were documented by FT-IR (Figure 1) and XPS (Figure 2) spectroscopic analysis of each of the plasma generated polymeric films. The FT-IR spectra confirm the presence of the key functional groups of interest. These are identified as amines from the N-H stretch of the peak at  $\sim 3400\text{ cm}^{-1}$  from  $\text{NH}_2\text{CH}_2\text{CH}_2\text{NH}_2$  (Fig. 1A); fluorocarbons from the C-F stretch at  $\sim 1200\text{ cm}^{-1}$  from  $\text{C}_6\text{F}_{14}$  (fig. 1B); hydroxyls from the O-H stretch at  $\sim 3500\text{ cm}^{-1}$  from EO2V (Fig. 1C) and carboxylic acid groups from the very broad stretching band, extending from  $\sim 3600$  to  $2500\text{ cm}^{-1}$ , characteristic of solid state –COOH groups, obtained from the VAA (Fig. 1D) [45]. Additional features of these spectra are consistent with those anticipated from plasma generated polymer films and include the presence of a cyano group at  $2200\text{ cm}^{-1}$  and imine at  $1600\text{ cm}^{-1}$  as generated by the energetic RF discharge conditions employed (Fig. 1a) and generally observed in plasma films from amine containing monomers. The added bands in the poly EO2V spectrum at  $2900$  and  $1100\text{ cm}^{-1}$  are consistent with the presence of C-H and C-O stretching vibrations, both of which are present in the starting monomer. The sharp peak at  $1700\text{ cm}^{-1}$  in the VAA spectrum is the expected carbonyl stretch associated with the presence of the –COOH groups.

The high resolution C(1s) XPS spectra, shown in Figure 2, provide added confirmation of the chemical compositions of these films. The XPS spectra are presented in the same order as employed for the FT-IR results shown in Figure 1. For each sample, the films were neutralized during data acquisition and the C(1s) binding energy of carbon atoms not bound to a heterogeneous atom was set at 284.6 eV. The results from the ethylenediamine film are consistent with the presence of C-N bonds (285.8 eV) as well as somewhat higher bonding energy peaks attributable to the C=N and cyano groups and a partially oxidized group, such as N-C-O (at 289 eV), reflecting a small degree of post plasma spontaneous oxidation of the films. The fluorocarbon film reveals the dominant presence of  $\text{CF}_2$  groups (at 291 eV) along with contributions from  $\text{CF}_3$  (at 293 eV), C-F (287.5 eV) and C atoms beta to C-F bonds at 285 eV. The EO2V spectrum shows the dominant presence of C-C (284.6 eV) and C-O (286eV) bonding along with a small contribution of higher oxidized group such as C=O. The VAA spectrum is consistent with the presence of C-C and COOH groups (289 eV) with a small contribution from C-O bonds. The assignment of the various binding energies noted above are consistent with literature values for these functionalities.[46] Table 2 provides the atom percent composition of the films employed in this study, as obtained from the XPS results. The percent hydrogen atoms in these films is not included since it is not obtainable from the XPS data.

### Surface functionality influences fibrotic capsule formation

H&E stain of the 2-week implants clearly show that particles bearing different functionality prompt significantly different extents of biomaterial-mediated fibrotic reactions (Figure 3). The degrees of fibrotic reactions are represented by three parameters, namely: capsule thickness, capsule cell density, and cell infiltration into particle implants (Figure 3).

First, the implant surrounding tissue capsule varied between all the samples, with -OH group functionality showing the highest thickness, namely  $251.0 \pm 45.6\ \mu\text{m}$ . Microsphere implants

with  $-\text{NH}_2$  groups prompt slightly less capsule formation, with average capsule thickness of  $151.7 \pm 35.3 \mu\text{m}$ . On the other hand, particles with  $-\text{COOH}$  groups elicited a dramatically decreased capsule formation of only  $23.4 \pm 2.8 \mu\text{m}$  (Figure 2.A.). Medium fibrotic tissue formation was found in tissue surrounding particles bearing  $-\text{CF}_x$ - functional group and the uncoated polypropylene control particles, having mainly  $-\text{CH}_2$ - functionality, where the average thicknesses of fibrotic capsules were  $101.3 \pm 35.9$  and  $55.3 \pm 10.5 \mu\text{m}$ , respectively (Figure 4.A.). These initial results reveal that the chemical nature of the surface of a subcutaneous implant modulates the thickness of the fibrous capsule that is organized around the implant. The extent of this tissue response is influenced by the functional groups as it does not correlate simply with surface hydrophilicity.

### Surface functionality affect cell infiltration into particle implants

Second, rather unexpectedly, we have observed that microspheres with different surface functional groups also prompt different extent of cell penetration into the particle implants. In general, functionality which triggers the stronger fibrotic reactions also prompts deeper cellular penetration (Figure 4.B.). Specifically, particle implants with  $-\text{OH}$  hydrophilic group on the surface showed the highest infiltration length ( $911 \pm 188 \mu\text{m}$ ). Particles with  $-\text{NH}_2$ ,  $-\text{CH}_2$ ,  $-\text{CF}_x$  show moderate cell penetrations with infiltration length  $320 \pm 57 \mu\text{m}$ ,  $189 \pm 34 \mu\text{m}$ , and  $203 \pm 46 \mu\text{m}$ , respectively (Figure 4. B). As expected, in light of the fibrotic capsule formation noted above, particles with the  $-\text{COOH}$  group exhibited the least infiltration inside particle implants, only ( $87 \pm 45 \mu\text{m}$ ) (Figure 2.B). These results show that surface functionality not only affect cell accumulation outside but also immigration into the implants.

### Surface functionality modulates CD11+ inflammatory cell recruitment

To determine the distribution of inflammatory cells and their spatial relationship to fibrotic tissue and surface functionality, we quantified the numbers of CD11b+ inflammatory cells (Figure 5). Interestingly, we find large differences in the extent of inflammatory cell recruitment by the different surfaces in an order roughly similar to the trend found in fibrotic reactions, i.e.  $-\text{NH}_2 > -\text{OH} > -\text{CF}_x > -\text{CH}_2 > -\text{COOH}$  (Figure 4). Generally speaking, the accumulation of CD11b+ inflammatory cells can be categorized into three groups. First, particle implants with  $-\text{NH}_2$  and  $-\text{OH}$  functional group trigger strong recruitment of CD11b+ inflammatory cells. It is observed that the number of inflammatory cells at the capsule for  $-\text{NH}_2$  shows the maximum, with a cell number of  $261 \pm 39.35$  CD11b+ cells per field of view (Figure 6); the  $-\text{OH}$  surfaces follow with a cell number of  $135.25 \pm 36.86$  CD11b+ cells per field of view. Secondly, implants with  $-\text{CF}_x$ - and  $-\text{CH}_2$ - functional groups trigger moderate inflammatory cell accumulation. Tissue capsules surrounding particles bearing  $-\text{CF}_x$ - show a cell count of  $50.25 \pm 12.03$  CD11b+ cells per field of view. The polypropylene control particles with  $-\text{CH}_2$ - functionality show a cell count of  $26.25 \pm 8.13$  CD11b+ cells per field of view. Finally, particle implants with  $-\text{COOH}$  elicit the least inflammatory responses with CD11b+ cell count of only  $11.75 \pm 1.5$  cells per field of view (Figure 6).

### Correlation between fibrotic capsule thickness and cell infiltration depth

To validate the relationship between surface functionality-mediated inflammatory responses and fibrotic reactions, we carried out linear regression between inflammatory responses (CD11b+ cell numbers) and fibrotic reactions (capsule thickness and cell infiltration depth). Interestingly, we find a strong correlation between capsule thicknesses and cell infiltration depth (Figure 7A). In contrast, CD11b+ cell numbers correlate poorly with both capsule thickness (Figure 7B) and cell infiltration depth (Figure 7C). Clearly, these results suggest indicate that the inflammatory cell numbers alone is insufficient to predict the degree of implant-mediated fibrotic reactions.

## DISCUSSION

The formation of fibrotic capsule surrounding implants often lead to the failure of implants, including drug release devices, encapsulated cells, and implantable sensors.[2–6] It is generally believed that, by reducing biomaterial-mediated fibrotic reactions and the formation of collagenous diffusion barrier, the drug release properties and sensor sensitivity and life-span would be substantially improved.[2–6, 47–49] An extensive body of in vitro evidence indicates that the surface chemical composition of biomaterials may modify cell adhesion, activation and the secretion of cytokines/fibrogenic factors.[29–31,50,51] We, and others, have previously observed that plasma functionalized surfaces exert different affinity to fibrinogen and the extent of fibrinogen denaturation correlates with the degree of biomaterial-mediated accumulation of inflammatory cells, including neutrophils and macrophages/monocytes.[26,32,33] However, the effect of surface functionality on long-term fibrotic reactions is rather unimpressive.[26,36] As a result, investigators have assumed that surface functionality has little influence on fibrotic reactions.[34,35].

The results of the present study suggest that the reported ineffectiveness of surface functionality in altering long-term fibrotic reactions may very well be caused by lack of direct interaction between fibrotic cells and surface functional groups. Since only the initially arriving cells have direct contact with the implant surfaces and their functional groups, it seems likely that, by increasing the available functionalized surface area, the effect of surface functional groups on tissue responses may be greatly enhanced. Such large surface area to volume ratio can be found on both porous scaffold and drug release microspheres.

Indeed, the results obtained support the basic concept that with increasing surface to volume ratio of the implant, the nature of the surface functional groups strongly influences fibrotic tissue reactions. The actual tissue response appears to be strongly dependent on the nature of the functional group, and not simply the relative magnitude of the overall surface hydrophilicity/hydrophobicity. Specifically, surface  $-NH_2$  and  $-OH$  group prompt the strongest inflammatory cell accumulation and fibrotic capsule formation. Surface  $-NH_2$  has been shown to enhance protein adsorption and denaturation.[26,52] The accumulation of a large amount of denatured fibrinogen on  $-NH_2$  functional group rich surfaces may serve as a strong signal for recruiting inflammatory cells and promoting fibrotic tissue formation.[26] The strong tissue responses to  $-OH$  rich particles are unexpected. It is well established that  $-OH$  coating reduces protein adsorption and cell adhesion.[50] The poor blood and tissue compatibility to polyethylene glycol coated surfaces have also been documented.[53,54] Although the detailed mechanism of hydroxyl group mediated tissue reactions has yet to be determined, we believe that  $-OH$  containing surfaces obtained from the EO2V monomer. [41,55], which are very similar in structure to polyethylene glycol and tetraglyme surfaces, [35] may prompt the conformational changes of fibrinogen resulting in denatured fibrinogen on implants with surrounding tissue thus prompting the subsequent inflammatory and fibrotic reactions. Functional groups of  $-CF_x-$  and  $-CH_2-$  generated only moderate inflammatory and fibrotic reactions. The fluorocarbon coatings are extremely hydrophobic. In an acute inflammatory animal model, these fluorocarbon surfaces were observed to adsorb and to denature fibrinogen only to a moderate extent [26], which correlates well with in vivo inflammatory cell accumulation of the present study. The  $-CH_2-$  group on uncoated polypropylene particles also prompts only moderate tissue response. This would appear to be in agreement with other studies which have related foreign body reactions to most of the commonly used biomaterials, such as polyethylene terephthalate.[26,36,56] Rather surprisingly, we find the  $-COOH$  functional group elicits minimal inflammatory reactions and fibrotic tissue formation. It is not clear how surface  $-COOH$  group diminishes foreign

body reactions. However, the biocompatible properties of –COOH group should be explored for improving the safety and utility of medical devices.

To the best of our knowledge, this study represents the first documented observations that in vivo tissue compatibility may be modified by varying surface chemistry on microspheres. Furthermore, the results suggest the surface/volume ratio of the implant may play an important role in influencing the importance of surface chemistry on tissue responses and/or compatibility. The results obtained from this study may help improve the function and safety of many medical devices, such as drug release devices, encapsulated cells and implantable sensors.

## Acknowledgments

This work was supported by NIH grants RO1 GM074021, and an AHA Established Investigator Award.

## References

1. Zhao Q, Agger MP, Fitzpatrick M, Anderson JM, Hiltner A, Stokes K, Urbanski P. Cellular interactions with biomaterials: in vivo cracking of prestressed. Pellethane 2363-80A. *J Biomed Mater Res.* 1990; 24:621–637. [PubMed: 2324131]
2. Ratner BD. Reducing capsule thickness and enhancing angiogenesis around implant drug releasing systems. *J Controlled Release.* 2002; 78:211–218.
3. Fournier E, Passirani C, Montero-Menei CN, Benoit JP. Biocompatibility of implantable synthetic polymeric drug carriers: focus on brain compatibility. *Biomaterials.* 2003; 24:3311–3331. [PubMed: 12763459]
4. Rihova B. Immunocompatibility and biocompatibility of cell delivery systems. *Adv Drug Delivery Rev.* 2000; 42:65–80.
5. Soon-Shiong P, Otterlie M, Skjak-Braek G, Smidsrod O, Heintz R, Lanza RP, Espevik T. An immunologic basis for the fibrotic reactions to implanted microcapsules. *Transplant Proc.* 1991; 23:758–759. [PubMed: 1990681]
6. Colton CK. Implantable bihybrid artificial organs. *Cell Transplant.* 1995; 4:415–436. [PubMed: 7582573]
7. Butler K, Benghuzzi H, Tucci M, Cason Z. A comparison of fibrous tissue formation surrounding intraperitoneal and subcutaneous implantation of ALCAP, HA, and TCP ceramic devices. *Biomed Sci Instrum.* 1997; 34:18–23. [PubMed: 9603006]
8. Amon M, Menapace R, Radax U, Papapanos P. Clinical results with three different kinds of small optic PMMA IOLs. *Int Ophthalmol.* 1994; 18:9–13.
9. Amon M, Menapace R. Long-term results and biocompatibility of heparin surface modified intraocular lenses. *J Cataract Refract Surg.* 1993; 19:258–262. [PubMed: 8487171]
10. Nishi O, Nishi K, Sakka Y, Sakurba T, Maeda S. Intercapsular cataract surgery with lens epithelial cell removal. Part IV: Capsular fibrosis induced by poly (methylmethacrylate). *J Cataract Refract Surg.* 1991; 17:471–477.
11. Lindsay R. Blood surface interactions. *Trans Am Soc Artif Organs.* 1980; 26:603–610.
12. Leninger RI, Hutson TB, Jackson RJ. Spectroscopic approaches to the investigation of interactions between artificial surfaces and proteins. *Ann NY Acad Sci.* 1978; 516:173–183.
13. Kuwahara T, Markert M, Wauters JP. Protein adsorption on dialyzer membranes influences their biocompatibility properties. *Contrib Nephrol.* 1989; 74:52–57. [PubMed: 2562019]
14. Sevastianov VI. Role of protein adsorption in blood compatibility of polymers. *CRC Crit Rev Biocomp.* 1988; 4:109–154.
15. Bohnert JL, Horbett TA. Changes in adsorbed fibrinogen and albumin interactions with polymers indicated by decreases in detergent elutability. *Journal of Colloid and Interface Science.* 1986; 111:363–377.
16. Horbett TA. Principles underlying the role of adsorbed plasma proteins in blood interactions with foreign materials. *Cardiovasc Pathol.* 1993; 2:137S–148S.



17. Shinoda BA, Mason RG. Reaction of blood with artificial surfaces of hemodialyzers. Studies of human blood with platelet defects or coagulation factor deficiencies. *Biomater Med Devices Artif Organs*. 1978; 6:305–329. [PubMed: 312115]
18. Zhao Q, Topham N, Anderson JM, Hiltner A, Lodoen G, Payet CR. Foreign-body giant cells and polyurethane biostability: in vivo correlation of cell adhesion and surface cracking. *J Biomed Mater Res*. 1991; 25:177–183. [PubMed: 2055915]
19. Anderson JM, Bonfield TL, Ziats NP. Protein adsorption and cellular adhesion and activation on biomedical polymers. *Int J Artif Org*. 1990; 13:375–382.
20. Lee JH, Park JW, Lee HB. Cell adhesion and growth on polymer surfaces with hydroxyl groups prepared by water vapor plasma treatment. *Biomaterials*. 1991; 12:443–448. [PubMed: 1892978]
21. Lee JH, Jung HW, Kang IK, Lee HB. Cell behavior on polymer surfaces with different functional groups. *Biomaterials*. 1994; 12:705–711. [PubMed: 7948593]
22. Panchalingam V, Chen X, Huo HH, Savage CR, Timmons RB, Eberhart RC. Pulsed plasma discharge polymer coatings. *ASAIO J*. 1993; 39:M305–309. [PubMed: 8268548]
23. Panchalingam V, Poon B, Huo HH, Savage CR, Timmons RB, Eberhart RC. Molecular surface tailoring of biomaterials via pulsed RF plasma discharges. *J Biomater Sci Polym Ed*. 1993; 5:131–145. [PubMed: 8297826]
24. Sano S, Kato K, Ikada Y. Introduction of functional groups onto the surface of polyethylene for protein immobilization. *Biomaterials*. 1993; 14:817–822. [PubMed: 8218735]
25. Sheu MS, Hoffman AS, Feijen J. A glow discharge treatment to immobilize poly (ethylene oxide)/poly (propylene oxide) surfactants for wettable and nonfouling biomaterials. *J Adhesion Sci Technol*. 1992; 6:995–1009.
26. Tang L, Wu Y, Timmons RB. Fibrinogen adsorption and host tissue responses to plasma functionalized surfaces. *J Biomed Mater Res*. 1998; 42:156–63. [PubMed: 9740018]
27. Desai NP, Hubell JA. Tissue response to intraperitoneal implants of polyethylene oxide-modified polyethylene terephthalate. *Biomaterials*. 1992; 13:505–510. [PubMed: 1385984]
28. Christenson L, Aebischer P, McMillan P, Galletti PM. Tissue reaction to intraperitoneal polymer implants: Species difference and effects of corticoids and doxorubicin. *J Biomed Mater Res*. 1989; 23:705–718. [PubMed: 2661559]
29. Sperling C, Schweiss RB, Streller U, Werner C. In vitro hemocompatibility of self-assembled monolayers displaying various functional groups. *Biomaterials*. 2005; 26:6547–6557. [PubMed: 15939466]
30. Pompe T, Keller K, Mothes G, Nitschke M, Teese M, Zimmermann R, Werner C. Surface modification of poly(hydroxybutyrate) films to control cell-matrix adhesion. *Biomaterials*. 2007; 28:28–37. [PubMed: 16963116]
31. Keselowsky BG, Collard DM, Garcia AJ. Surface chemistry modulates focal adhesion composition and signaling through changes in integrin binding. *Biomaterials*. 2004; 25:5947–5954. [PubMed: 15183609]
32. Barbosa JN, Barbosa MA, Augas AP. Inflammatory response and cell adhesion to self-assembled monolayers of alkanethiolates on gold. *Biomaterials*. 2004; 25:2557–2563. [PubMed: 14751741]
33. Barbosa JN, Madureira P, Barbosa MA, Aguas AP. The attraction of Mac-1+ phagocyte during acute inflammation by methyl-coated self-assembled monolayers. *Biomaterials*. 2005; 26:3021–3027. [PubMed: 15603797]
34. Ratner BD, Bryant SJ. Biomaterials: where we have been and where we are going. *Ann Rev Biomed Eng*. 2004; 6:41–75. [PubMed: 15255762]
35. Shen M, Martinson L, Wagner MS, Castner DG, Ratner BD, Horbett TA. PEO-like plasma polymerized tetraglyme surface interactions with leukocytes and proteins; in vitro and in vivo studies. *J Biomater Sci Polym Ed*. 2002; 13:367–390. [PubMed: 12160299]
36. Barbosa JN, Madureira P, Barbosa MA, Aguas AP. The influence of functional groups of self-assembled monolayers on fibrous capsule formation and cell recruitment. *J Biomed Mater Res*. 2006; 26A:737–743.
37. Susut C, Timmons RB. Plasma enhanced chemical vapor depositions to encapsulate crystals in thin polymeric films: a new approach to controlling drug release rates. *Inter J Pharmaceutics*. 2005; 288:253–261.

38. Cho J, Denes FS, Timmons RB. Plasma Processing Approach to Molecular Surface Tailoring of Nanoparticles: Improved Photocatalytic Activity of TiO<sub>2</sub>. *Chem Mater*. 2006; 18:2989–2996.
39. Savage CR, Lin JW, Timmons RB. Molecular control of surface film compositions via pulsed RF plasma polymerization of perfluoropropylene oxide. *Chem Mater*. 1991; 3:575–581.
40. Rinsch CL, Chen X, Panchalingam V, Eberhart RC, Wang JH, Timmons RB. Pulsed radio frequency plasma polymerization of allyl alcohol: controlled deposition of surface hydroxyl groups. *Langmuir*. 1996; 12:2995–3002.
41. Wu Y, Timmons RB, Jen JS, Molock FE. Non-fouling surfaces produced by gas phase pulsed plasma polymerization of an ultra low molecular weight ethylene oxide containing monomer. *Colloids Surf B: Biointerfaces*. 2000; 18:235–248. [PubMed: 10915946]
42. Harsch A, Calderon J, Timmons RB, Gross GW. Pulsed plasma deposition of allylamine on polysiloxane: a stable surface for neuronal cell adhesion. *J Neurosci Methods*. 2000; 98:135–144. [PubMed: 10880827]
43. Zhang Z, Menges B, Timmons RB, Knoll W, Forch R. Surface plasmon resonance studies of protein binding on plasma polymerized di(ethylene glycol) monovinyl ether films. *Langmuir*. 2003; 19:4765–4770.
44. Li M, Timmons RB, Kinsel GR. Radio frequency plasma polymer coatings for affinity capture MALDI mass spectrometry. *Anal Chem*. 2005; 77:350–353. [PubMed: 15623315]
45. Socrates, G. *Infrared Characteristic Group Frequencies*. 2. John Wiley and Sons; New York: 1994.
46. Beamson, G.; Briggs, D. *High Resolution XPS of Organic Polymers – The Scienta ESCA300 Database*. John Wiley & Sons; 1992.
47. Sharkawy AA, Klitzmann B, Truskey GA, Reichert WM. Engineering the tissue which encapsulates subcutaneous implants. I. Diffusion properties. *J Biomed Mater Res*. 1997; 37:401–412. [PubMed: 9368145]
48. Wood RC, LeCluyse EL, Fix JA. Assessment of a model for measuring drug diffusion through implant-generated fibrous capsule membranes. *Biomaterials*. 1995; 16:957–959. [PubMed: 8562786]
49. Anderson JM, Niven H, Pelagalli J, Olanoff LS, Jones RD. The role of the fibrous capsule in the function of implanted drug-polymer sustained release systems. *J Biomed Mater Res*. 1981; 15:889–902. [PubMed: 7309770]
50. Barbosa JN, Madureira P, Barbosa AM, Aguas PA. The influence of functional groups of self-assembled monolayers on fibrous capsule formation and cell recruitment. *J Biomed Mater Res*. 2006; 76A:737–743.
51. Thomsen P, Gretzer C. Macrophage interactions with modified materials surfaces. *Curr Opin Solid State Mater Sci*. 2001; 5:163–176.
52. Evans-Nguyen KM, Tolles LR, Gorkun OV, Lord ST, Schoenfisch MH. Interactions of thrombin with fibrinogen adsorbed on methyl-, hydroxyl-, amine-, and carboxyl-terminated self-assembled monolayers. *Biochemistry*. 2005; 44:15561–15568. [PubMed: 16300405]
53. Gorbet MS, Sefton MV. L Leukocyte activation and leukocyte procoagulant activities after blood contact with polystyrene and polyethylene glycol-immobilized polystyrene beads. *J Lab Clin Med*. 2001; 137:345–355. [PubMed: 11329532]
54. Gorbet MS, Sefton MV. Material-induced tissue factor expression but not CD11b upregulation depends on the presence of platelets. *J Biomed Mater Res*. 2003; 67:792–800.
55. Wu Y, Han LM, Thomes BE, Qiu H, Lee WW, Timmons RB. Pulsed plasma polymerizations: film chemistry control and applications. *Mater Res Soc Symposium Proceedings*. 1999; 77:544.
56. Hu WJ, Eaton JW, Tang L. Molecular basis of biomaterial-mediated foreign body reactions. *Blood*. 2001; 98:1231–1238. [PubMed: 11493475]

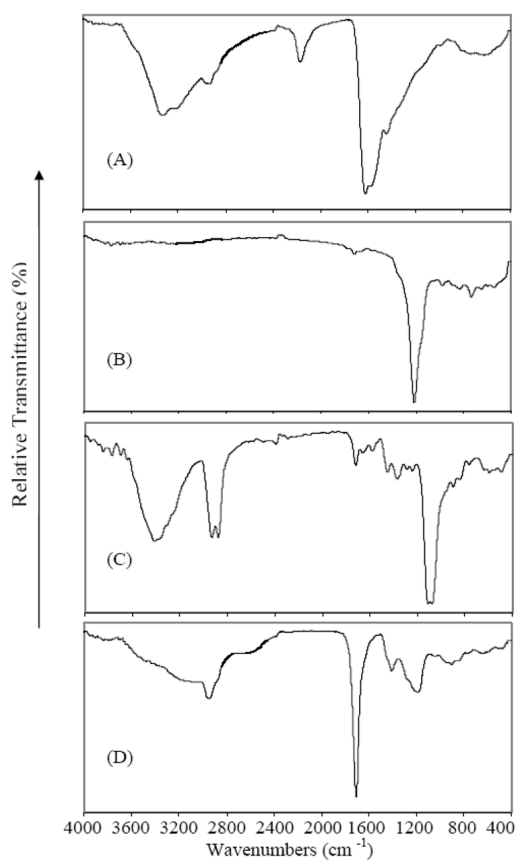


**Figure 1.** FT-IR spectra of polymeric films obtained from the plasma polymerization of ethylenediamine (A); hexafluorohexane (B), diethyleneglycol vinyl ether (C), vinyl acetic acid (D).

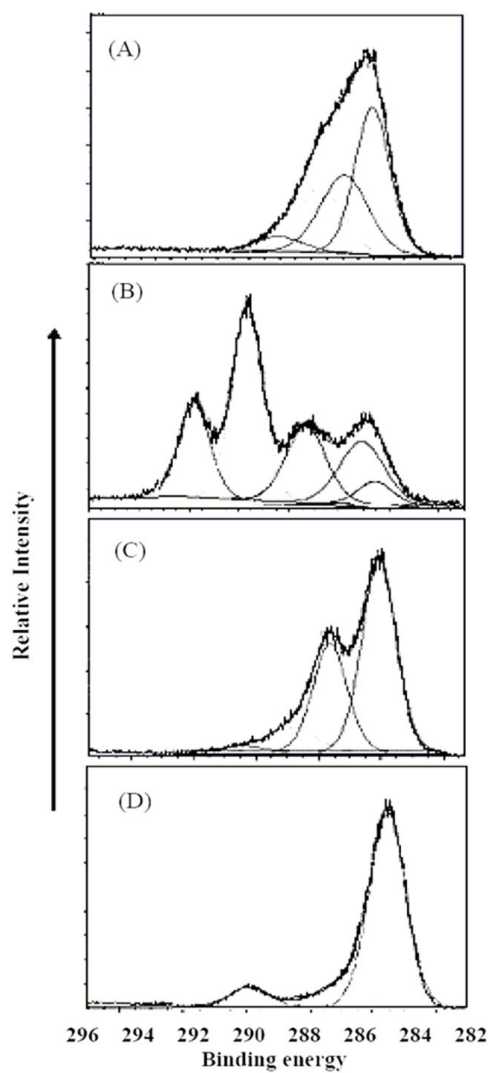


**Figure 2.** High resolution C(1s) XPS of the four plasma generated polymer films arranged in the same monomer order as presented in Figure 1.

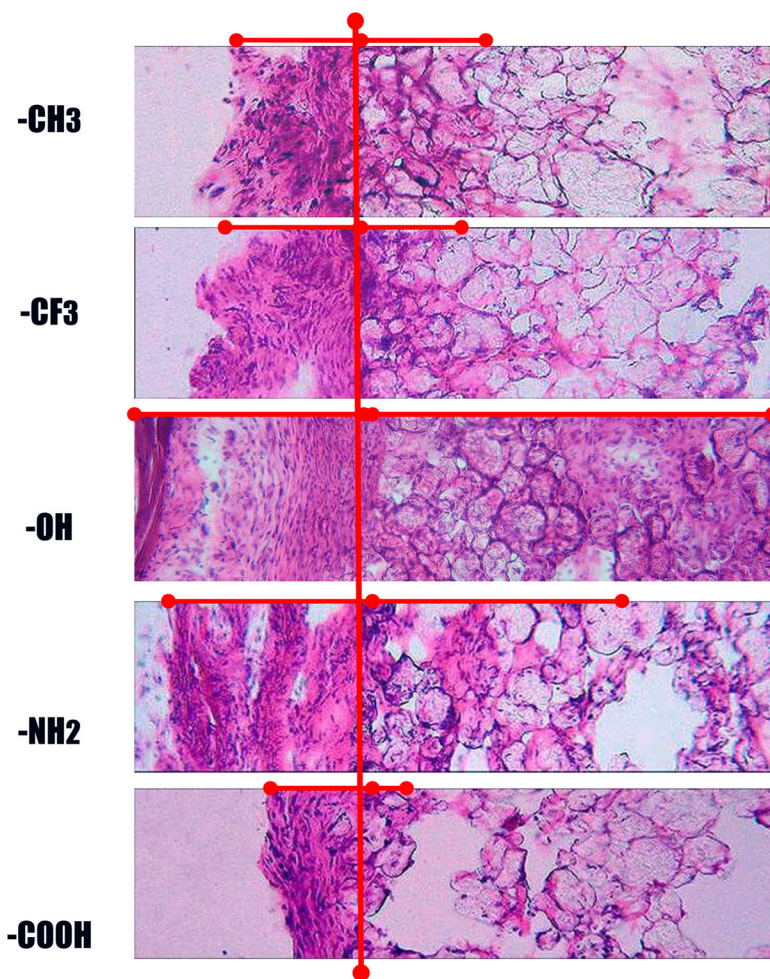


**Figure 3.** Implant-induced tissue responses were assessed based on capsule thickness and cellular infiltration. H&E stain of 2 week old skin tissue loaded with implant with different surface functionalities. The presence of capsule and cell infiltration (marked by -----) represents the fibrotic response at the implant, for  $-\text{CH}_2$ ,  $-\text{CF}_x$ ,  $-\text{OH}$ ,  $-\text{NH}_2$  and  $-\text{COOH}$  (Magnification 20x).

FIGURE 4.A.

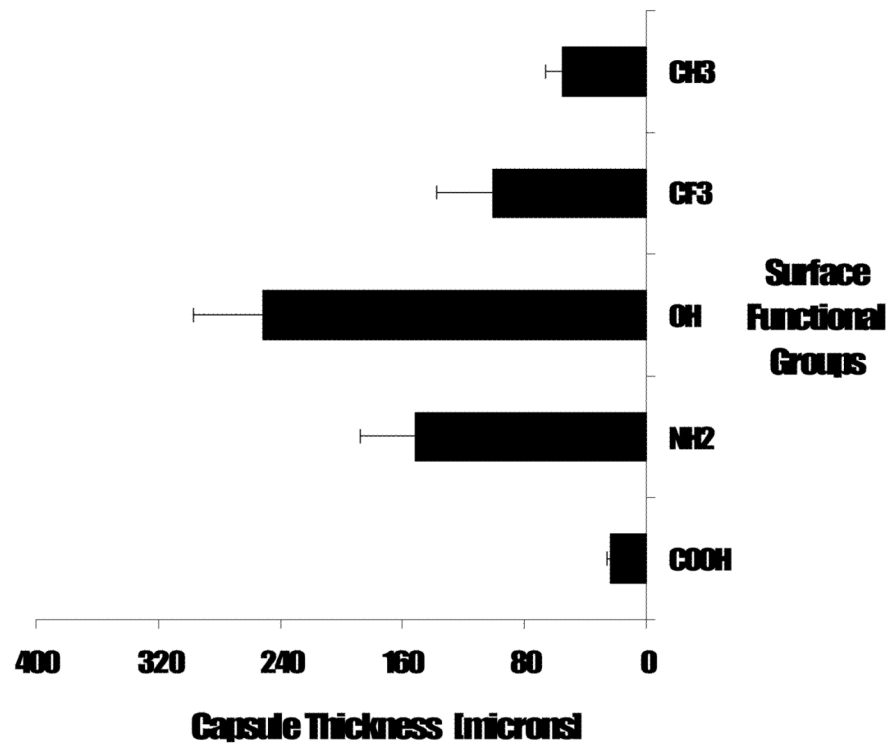
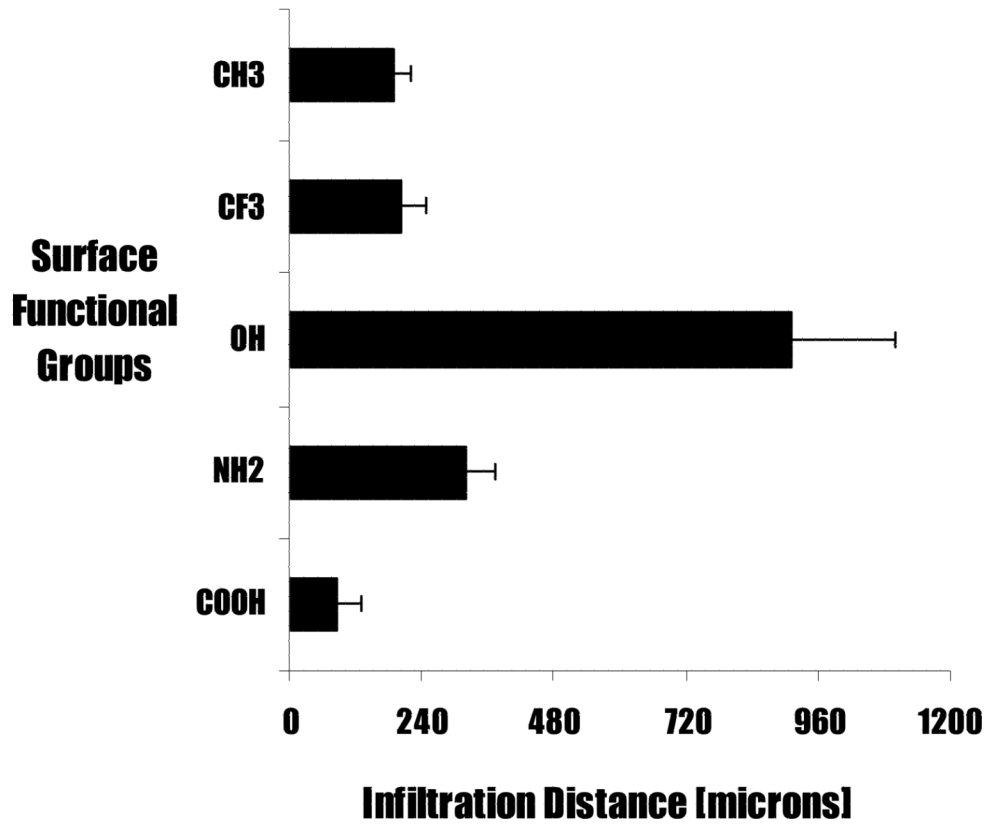
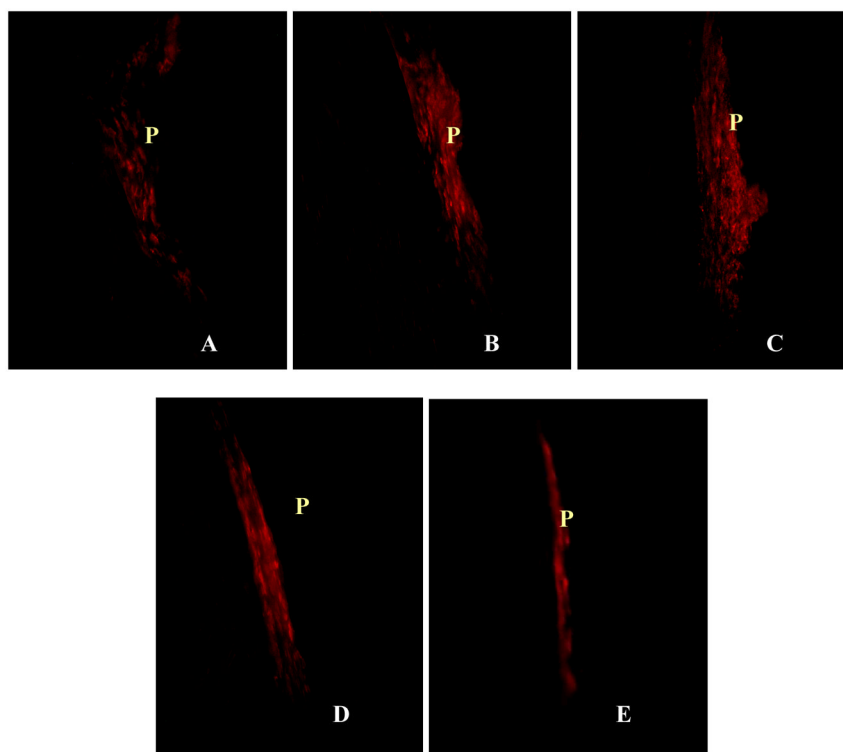


FIGURE 4. B.



**Figure 4.** Extent of tissue responses to variously treated particles were assessed based (A) capsule thickness and (B) cell infiltration distance into particle implants. Polypropylene (PP) coated with different surface functionalities were subcutaneously implanted in Balb/C mice. The animals were sacrificed at 2 weeks post implantations. Values shown reflect the average thickness of the capsule. Vertical lines denote  $\pm 1$  SD ( $n=4$  for  $-\text{CH}_2$ ,  $-\text{NH}_2$ ,  $-\text{OH}$ ,  $-\text{CF}_x$  and  $-\text{COOH}$ ).



**Figure 5.** Immunohistochemical analyses of the recruitment of CD11b + inflammatory cells to particle implants. Immunohistochemical staining of particle implants and surrounding tissues showing the presence of CD11b + inflammatory cells at the capsule triggered by the particles implant (P) with different surface functional groups, including control -CH<sub>2</sub> (A), -CF<sub>x</sub> (B), -OH (C), -NH<sub>2</sub> (D) and -COOH (E) (Magnification 40x).



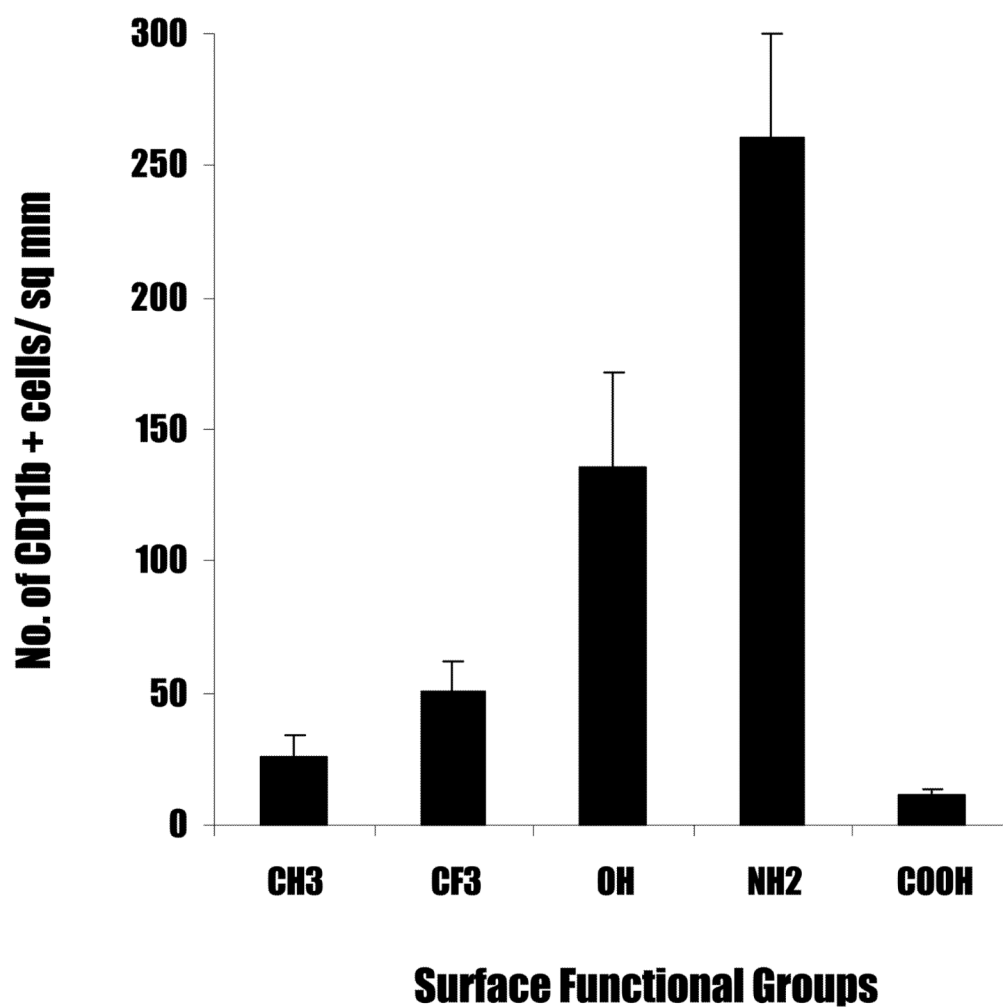


**Figure 6.** Accumulation of CD11b + cells at the capsule highest for cationic surfaces. Polypropylene particles coated with different surface functionalities were subcutaneously implanted in Balb/C mice. The animals were sacrificed at 2 weeks post implantations. Values shown reflect the average number of CD11b+ cells seen at the capsule for different surface functionalities. Vertical lines denote  $\pm 1$  SD ( $n = 4$  for  $-\text{CH}_2$ ,  $-\text{NH}_2$ ,  $-\text{OH}$ ,  $-\text{CF}_x$  and  $-\text{COOH}$ ).

FIGURE 7A

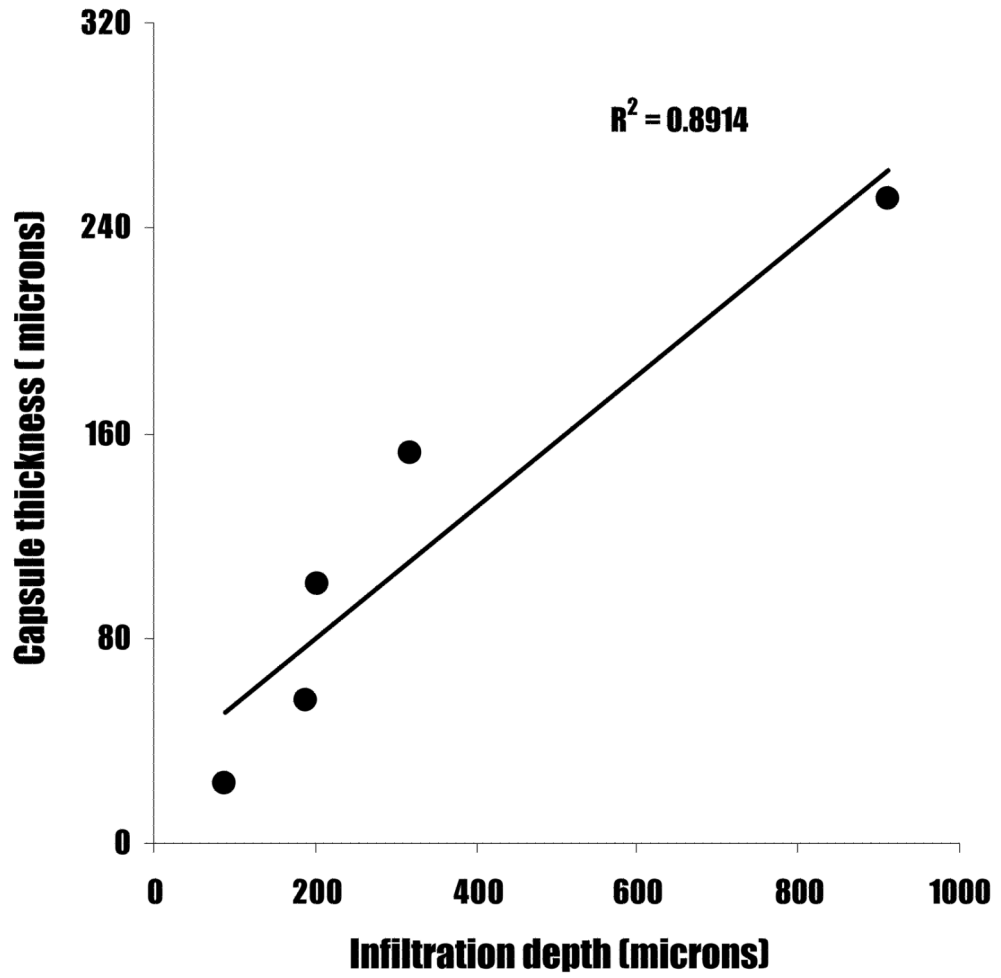


FIGURE 7B

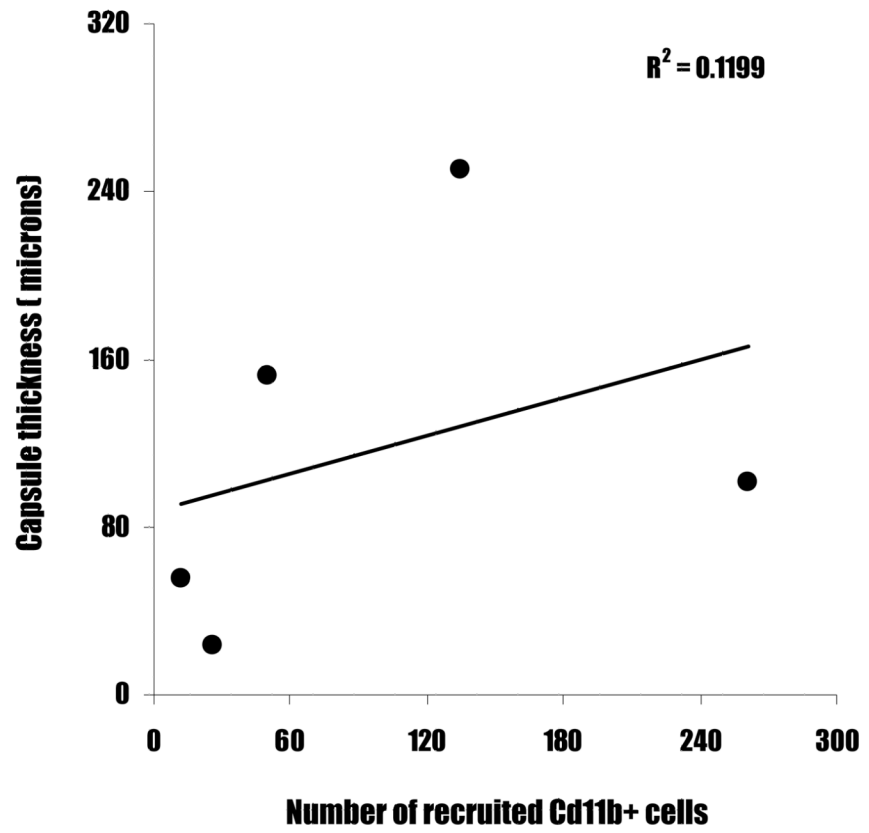
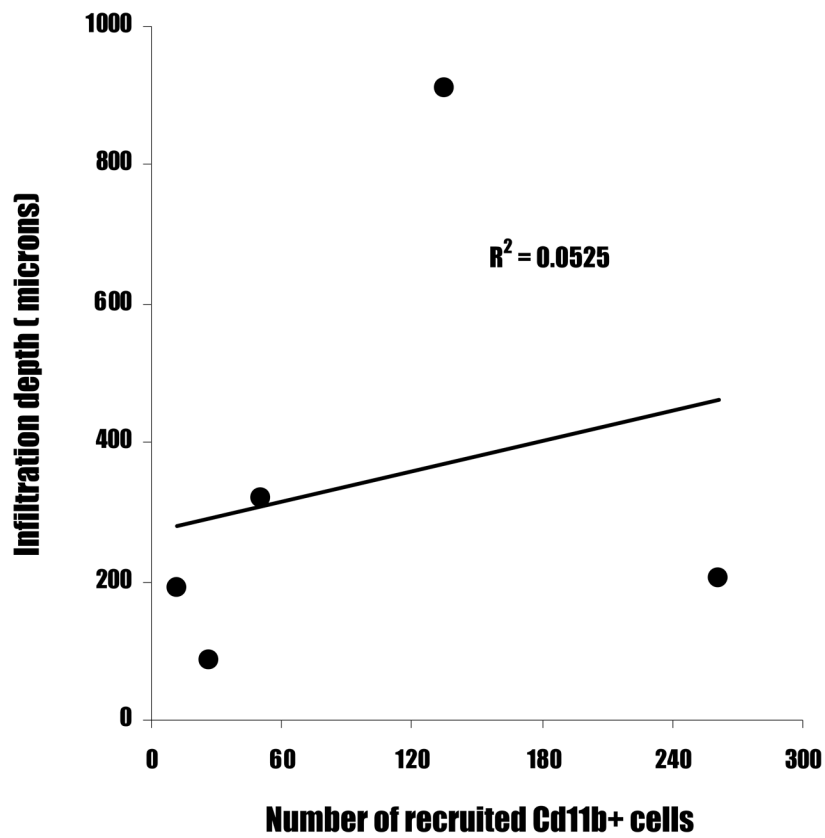


Figure 7C



**Figure 7.** The linear correlations between capsule thickness, CD11b+ cell number, and cell infiltration depth. (A) The capsule thicknesses are graphed against cell infiltration depth. (B) The cell infiltration depths are graphed against CD11b+ cell numbers. (C) The capsule thicknesses are graphed against CD11b+ cell numbers.

**Table 1**

Monomers and plasma conditions employed in depositing polymer films on the polypropylene particles.

| Monomer Name                       | Plasma Condition                | Water Contact Angle [Degree] | Surface Chemistry | Nature of surface    |
|------------------------------------|---------------------------------|------------------------------|-------------------|----------------------|
| Di (ethylene glycol) vinyl acetate | 20/300,33.7W, 60 mTorr,60 min   | 45                           | -OH               | Hydrophilic          |
| Ethylene diamine                   | 15/35, 200W, 78–80 mTorr, 15min | 12–14                        | -NH <sub>2</sub>  | Hydrophilic Cationic |
| Perfluro hexane                    | 25/200, 200W, 200 mTorr, 30 min | 135                          | -CF <sub>3</sub>  | Hydrophobic          |
| Vinyl acetic acid                  | 0.75/20, 200W, 80 mTorr, 15 min | 29–30                        | -COOH             | Hydrophilic Anionic  |

**TABLE 2**

Percent atomic compositions of the pulsed plasma polymerized films.

| Monomers                     | % C  | % O   | % N   | % F  |
|------------------------------|------|-------|-------|------|
| Ethylenediamine              | 72.2 | 4.4   | 23.4  | -    |
| Perfluorohexane              | 39.2 | 0.000 | 0.000 | 60.8 |
| Diethyleneglycol vinyl ether | 75.1 | 24.9  | 0.000 | -    |
| Vinyl acetic acid            | 78.3 | 21.7  | 0.000 | -    |